

Cite this: *Nanoscale*, 2015, **7**, 5803

Ligand-functionalized degradable polyplexes formed by cationic poly(aspartic acid)-grafted chitosan–cyclodextrin conjugates†

Hai-Qing Song,^{a,b,c} Rui-Quan Li,^{a,b,c} Shun Duan,^{b,c} Bingran Yu,^{b,c} Hong Zhao,^d Da-Fu Chen^e and Fu-Jian Xu^{*a,b,c}

Polypeptide-based degradable polyplexes attracted considerable attention in drug delivery systems. Polysaccharides including cyclodextrin (CD), dextran, and chitosan (CS) were readily grafted with cationic poly(aspartic acid)s (PAAs). To further enhance the transfection performances of PAAs-based polyplexes, herein, different types of ligand (folic acid, FA)-functionalized degradable polyplexes were proposed based on the PAAs-grafted chitosan–cyclodextrin conjugate (CCPE), where multiple β -CDs were tied on a CS chain. The FA-functionalized CCPE (*i.e.*, CCPE-FA) was obtained *via* a host–guest interaction between the CD units of CCPE and the adamantane (Ad) species of Ad-modified FA (Ad-FA). The resulting CCPE/pDNA, CCPE-FA/pDNA, and ternary CCPE-FA/CCPE/pDNA (prepared by layer-by-layer assembly) polyplexes were investigated in detail using different cell lines. The CCPE-based polyplexes displayed much higher transfection efficiencies than the CS-based polyplexes reported earlier by us. The ternary polyplexes of CCPE-FA/CCPE/pDNA produced excellent gene transfection abilities in the folate receptor (FR)-positive tumor cells. This work would provide a promising means to produce highly efficient polyplexes for future gene therapy applications.

Received 20th December 2014,
Accepted 21st February 2015

DOI: 10.1039/c4nr07515c

www.rsc.org/nanoscale

Introduction

Gene therapy depends on optimal delivery vectors with high transfection efficiency and low toxicity.^{1–5} Among numerous gene carriers, cationic polymers as a major type of nonviral delivery vectors have drawn much attention due to the advantages of safety, low host immunogenicity, large-scale preparation and potential cell targeting properties over viral vectors.^{6–10} Due to the unique properties of renewability, low cytotoxicity and excellent biocompatibility, polysaccharides are good candidates in the preparation of new drug delivery

systems. A variety of polysaccharides including cationic chitosan (CS),^{5,11–13} cyclodextrins (CDs),^{14–16} dextran,^{17,18} pullulan,¹⁹ chondroitin sulfate,²⁰ and hyaluronic acid²¹ were reported to be used for effective gene polyplexes.

Polypeptide-based degradable polyplexes attracted more attention in drug delivery systems.^{22,23} Due to its degradability and similar structures to polypeptides, polyamino acid was viewed as the best candidate for the development of new delivery vectors.^{24–26} Poly(aspartic acid)s (PAAs) prepared by the ring-opening reaction of β -benzyl-L-aspartate N-carboxy anhydride (BLA-NCA) could be aminolyzed to produce degradable polyplexes with high transfection and low cytotoxicity.^{24,27,28} More recently, we reported that polysaccharides including CD, dextran, and CS were readily grafted with aminolyzed PAAs side chains for efficient gene delivery.^{24,29,30} In comparison with linear cationic PAAs, the CD-cored star PAAs vectors exhibited better gene delivery performances.²⁴ The CD-cored PAAs vectors could also be assembled through the host–guest interactions with the PAAs backbones containing pendant benzene groups, producing supramolecular polyplexes.²⁹ However, it was found that CS-based polyplexes exhibited much higher gene transfection efficiencies than CD-cored ones.³⁰ Further enhancement in the transfection performances of degradable polyplexes is desirable to facilitate their applications.

^aState Key Laboratory of Chemical Resource Engineering, College of Materials Science & Engineering, Beijing University of Chemical Technology, Beijing 100029, China

^bBeijing Laboratory of Biomedical Materials, Beijing University of Chemical Technology, Beijing 100029, China. E-mail: xufj@mail.buct.edu.cn

^cKey Laboratory of Carbon Fiber and Functional Polymers (Beijing University of Chemical Technology), Ministry of Education, Beijing 100029, China

^dDepartment of Mechanical and Nuclear Engineering, Virginia Commonwealth University, Richmond, Virginia 23284, USA

^eLaboratory of Bone Tissue Engineering, Beijing Research Institute of Orthopaedics and Traumatology, Beijing JiShuiTan Hospital, Beijing, 100035, China

† Electronic supplementary information (ESI) available: ¹H NMR assay, synthetic route of Ad-FA, AFM images and cellular internalization rate can be found in ESI. See DOI: 10.1039/c4nr07515c

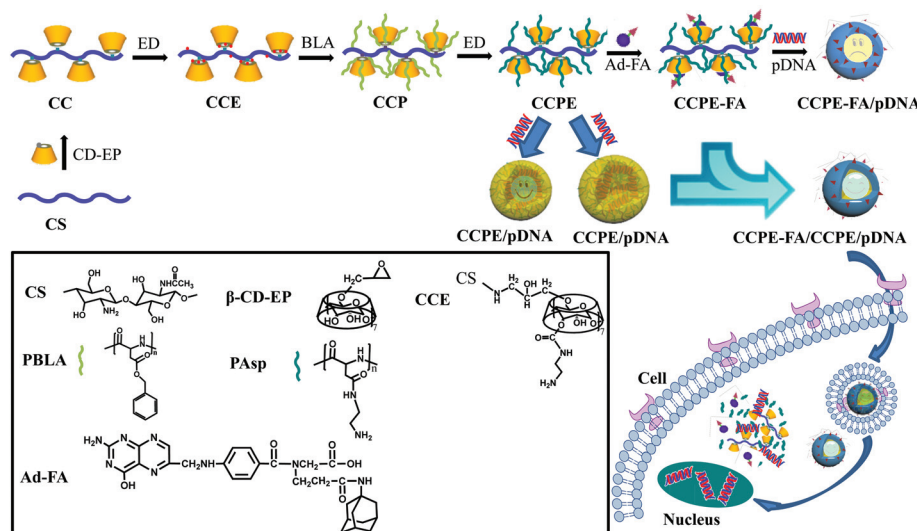


Fig. 1 Schematic diagram illustrating the preparation processes and cellular uptake of CCPE/pDNA, CCPE-FA/pDNA and CCPE-FA/CCPE/pDNA polyplexes.

Cell-targeting is also significant in drug delivery systems since targeting can reduce side effects and enhance delivery efficiency.^{5,7} Targeting ligands such as folic acid (FA) were widely employed for developing tumor cell-targeting delivery systems.^{5,7,31–33} A kind of folate receptor (FR) is overexpressed in cellular membranes of many cancer cells. To further enhance the transfection efficiencies and induce the tumor-targeting properties of PAsp-based polyplexes, in this work, different types of FA-functionalized PAsp polyplexes were proposed for a highly efficient gene delivery based on PAsp-grafted chitosan–cyclodextrin conjugates (CCPE), where multiple β-CDs containing hydrophobic central cavities as ligands were tied on a CS chain for self-assembly (Fig. 1). The FA-functionalized CCPE (*i.e.*, CCPE-FA) was obtained *via* a host-guest interaction between the CD units of CCPE and the adamantane (Ad) species of Ad-modified FA (Ad-FA). The resulting CCPE/pDNA, CCPE-FA/pDNA, and ternary CCPE-FA/CCPE/pDNA (prepared by layer-by-layer assembly) polyplexes were investigated systematically in different cancer cell lines through a series of experiments, which included pDNA condensation ability, degradability, cell viability, gene transfection ability, folate competition assay, and cellular internalization. This present study can provide useful information for constructing highly efficient degradable polyplexes.

Experimental section

Materials

Branched polyethylenimine (PEI, $M_w \sim 25\,000$ Da), β-cyclodextrin (β-CD, >98%), 1,1'-carbonyldiimidazole (CDI, 97%), triphosgene (>99%), anhydrous dimethyl sulfoxide (DMSO), anhydrous *N,N*-dimethylformamide (DMF), ethylenediamine (ED, >98%), and 1-amantadine hydrochloride (Ad, 98%) were

purchased from Sigma-Aldrich Chemical Co., St. Louis, MO. Chitosan (CS, degree of deacetylation ~55%, $M_n \sim 6100$, Table 1) was obtained from Jinan Haidebei Ltd, China. Folic acid dihydrate (FA, 97%) and epichlorohydrin (EP, 99%) were purchased from Alfa Aesar. Anhydrous 1,4-dioxane L-aspartic acid β-benzyl ester (BLA, >98%) was purchased from Tokyo Chemical Industry Co. Ltd, Japan. The monomer β-benzyl-L-aspartate N-carboxy anhydride (BLA-NCA) was prepared with the Fuchs–Farthing method as described in our earlier work.²⁴ Tetrahydrofuran (THF), acetic ether and *n*-hexane were dried over CaH₂ for about a week and distilled over fresh CaH₂ powder under a normal pressure. Other solvents were directly used without any treatment. Plasmid pRL-CMV encoding Renilla luciferase (Promega Co, Cergy Pontoise, France) and

Table 1 Characterization of the polymers

Samples	M_n^e (g mol ⁻¹)	PDI ^e	Monomer repeat units per side chain ^f
CS ^a	6.14×10^3	1.24	
CC ^b	1.06×10^4	1.15	
CCE ^c	1.17×10^4	1.36	
CCPE1 ^d	3.07×10^4	1.45	4
CCPE2 ^d	7.32×10^4	1.29	13
CCPE3 ^d	9.77×10^4	1.33	18

^a The degree of deacetylation of CS used in this work was about 55%, which was determined from ¹H NMR. ^b Synthesized using a molar ratio [CS]:[CD-EP] of 1:30 at 80 °C for 72 h. ^c Synthesized using a molar ratio [CC]:[CDI] of 1:25 at room temperature for 24 h, followed by adding excessive ED for another 48 h. ^d Synthesized using different molar feed ratios [amino group of CCE]:[BLA-NCA] at 50 °C in 8 mL of anhydrous DMSO for 72 h, followed by 12 h aminolysis. ^e Determined from GPC results. PDI = weight average molecular weight/number average molecular weight, or M_w/M_n . ^f Determined from M_n of CCPE, where one CCE initiator contained about 32 primary amine groups.

plasmid pEGFP-N1 encoding enhanced green fluorescent protein (EGFP) (BD Biosciences, San Jose, CA) were amplified in *Escherichia coli* and purified according to the supplier's protocol (Qiagen GmbH, Hilden, Germany). HeLa, C6 and HepG2 cell lines were purchased from American Type Culture Collection (ATCC, Rockville, MD). The cells with passage number 3 were used for gene transfection assay.

Preparation of chitosan–cyclodextrin conjugates (CCs)

As shown in Fig. 1, CCs were prepared by combining multiple epichlorohydrin-modified CDs (CD-EPs) with one CS backbone. CD-EP was prepared using similar procedures reported earlier.³⁴ β-CDs (1.5 g) were firstly dissolved in a mixture of 5 mL of DMSO and 5 mL of isopropyl alcohol. 12.5 mL of 1 M NaOH aqueous solution was then added into the solution, followed by the addition of 2 mL of epichlorohydrin. The reaction mixture was kept with stirring at room temperature under a nitrogen atmosphere for 48 h. The pH of the reaction solution was adjusted to about 7.0 with concentrated hydrochloric acid, and excess acetone was used to precipitate the reaction mixture. The raw CD-EP was dissolved in a small amount of deionized (DI) water and dialyzed against DI water (4 × 5 L) with a dialysis membrane (MWCO, 1000 Da) at room temperature for 4 h. Finally, about 1.1 g of CD-EP was collected by lyophilization.

For the preparation of CC, CD-EP (0.5 g) and CS (80 mg) were dissolved in 5 mL of H₂O. The resulting mixture was kept with continuous stirring at 80 °C for 72 h under a nitrogen atmosphere. CC (134 mg) was obtained by lyophilization after dialyzing against DI water (4 × 5 L) with a dialysis membrane (MWCO, 7000 Da) at room temperature for 48 h.

Preparation of ED-functionalized CC (CS-CD-NH₂, CCE)

As described in our previous work,³⁰ the primary amine group containing CCE initiator was synthesized *via* the reaction of hydroxyl groups of CC activated by CDI with excessive ED. In brief, to activate the hydroxyl groups of CC, a solution of CDI (160 mg in 1 mL of anhydrous DMSO) was added into 4 mL of CC (0.4 g) solution in anhydrous DMSO with a molar feed ratio [CC]:[CDI] of 1:25. After keeping the resulting mixture with stirring at room temperature under a nitrogen atmosphere for 24 h, excessive ED (1.7 mL) was added dropwise, and then the final mixture was stirred for additional 48 h. Excess acetone was used to precipitate the reaction mixture. Raw CCE products were dissolved in a small amount of DI water and dialyzed against DI water (4 × 5 L) with a dialysis membrane (MWCO, 3500 Da) at room temperature for 24 h. Finally, CCE (0.45 g) was collected by lyophilization.

Synthesis and aminolysis of CC-*graft*-PAsp (CCP)

CCP was synthesized *via* the ring-opening polymerization of BLA-NCAs prepared by the Fuchs–Farthing method initiated by the primary amino groups of CCE. To prepare CCPs with different molecular weights, molar feed ratios (1:30, 1:50, and 1:100) of [the amino group of CCE]:[BLA-NCA] were used. As described earlier,³⁰ a pre-determined amount of

BLA-NCA monomers in 4 mL of DMSO was introduced dropwise into a 4 mL DMSO solution containing CCE (0.1 g). The reaction solution was stirred under a nitrogen atmosphere for 72 h at 50 °C. The CCP products were obtained from the reaction mixture by precipitation with diethyl ether and were washed with diethyl ether at least twice before vacuum drying.

Aminolysis reaction of CCP was conducted in DMSO by addition of excess ED to produce the ED-functionalized CCP (CCPE) as reported earlier.³⁰ Briefly, CCP (0.6 g) was first dissolved in 5 mL of DMSO, and then ED (1.5 mL) was added. The reaction proceeded with stirring at room temperature for 12 h. The raw product obtained by precipitation with excess diethyl ether was dissolved in deionized water and dialyzed against deionized water (3 × 5 L) with a dialysis membrane (MWCO, 7000 Da) at room temperature for 8 h, prior to being freeze-dried. About 0.2 g of CCPE was obtained.

FA-functionalized CCPE (CCPE-FA)

For the preparation of CCPE-FA *via* host–guest interaction, Ad-modified FA (Ad-FA) was first prepared using the similar method reported earlier.³⁵ The synthetic route is shown in Scheme S1 (see ESI†). FA (0.5 g) was dissolved in 10 mL of DMF. Then, 1-ethyl-3-(3-dimethylaminopropyl) carbodiimide hydrochloride (EDAC, 146.1 mg) and *N*-hydroxysuccinimide (NHS, 130.4 mg) were added. The resulting mixture solution was kept with stirring at room temperature for 24 h under a nitrogen atmosphere. Adamantanamine hydrochloride (Ad-NH₂, 212.6 mg) was dissolved in 1 mL of DMF that contained 0.16 mL of triethylamine. The resulting solution was stirred for 4 h at room temperature to remove hydrochloride. Then the solution containing Ad-NH₂ was added into the solution containing FA, and kept for another 48 h. The final Ad-FA (about 0.25 g) product was obtained by precipitation with excess acetone and vacuum drying.

CCPE-FA was produced *via* a host–guest interaction of CCPE and Ad-FA. A molar feed ratio [CD units of CCPE]:[Ad units of Ad-FA] of 1:5 was used. CCPE (with 0.05 mmol of CD units) in 5 mL of H₂O was introduced into a flask containing Ad-FA suspensions (with 0.25 mmol of Ad units) in 5 mL of H₂O. The mixture was stirred for 12 h at room temperature and then centrifuged to remove excess Ad-FA. The resulting supernatant was freeze-dried to produce CCPE-FA.

Polymer characterization

Gel permeation chromatography (GPC) and nuclear magnetic resonance (NMR) spectroscopy were applied to determine molecular weights and chemical structures of polymers, respectively. GPC measurements of CC were performed on a Waters GPC system equipped with Waters Styragel columns, a Waters-2487 dual wavelength (λ) UV detector, and a Waters-2414 refractive index detector. DMSO was used as the eluent at a low flow rate of 1.0 mL min⁻¹ at 25 °C. Molecular weights of CS, CCE, and CCPE were measured on a YL9100 GPC system equipped with a UV/vis detector and Waters Ultrahydrogel 250TM and Ultrahydrogel LinearTM 7.8 × 300 mm columns. A pH 3.5 acetic buffer solution was used as the eluent at a low

flow rate of 0.5 mL min^{-1} at 25°C . The calibration curve was obtained by monodispersed PEG standards. GPC was also used to determine the molecular weights of degraded CCPEs which were dissolved in PBS with constantly stirring in a 37°C incubator. ^1H NMR spectra were measured by accumulation of 1000 scans at a relaxation time of 2 s on a Bruker ARX 400 MHz spectrometer, using d_6 -DMSO or D_2O as the solvent. Chemical shifts were referred to the solvent peak, $\delta = 2.50 \text{ ppm}$ or $\delta = 4.70 \text{ ppm}$, respectively.

Preparation and biophysical characterization of polyplexes

Polymers to pDNA ratios are expressed as molar ratios of nitrogen (N) in polymers to phosphate (P) in DNA (or as N/P ratios). All CCPE/pDNA and CCPE-FA/pDNA polyplexes with desired N/P ratios were formed by mixing equal volumes of polymer and pDNA solutions. Each mixture was shaken with a vortex and then kept for 30 min at room temperature. The ternary polyplexes of CCPE-FA/CCPE/pDNA were prepared by a layer-by-layer assembly (Fig. 1). In this work, before achieving a final N/P ratio of 20, the CCPE/pDNA pre-polyplexes with N/P ratios of 5, 10 and 15 were first prepared as normal. After 30 min incubation, a suitable amount of the solution containing CCPE-FA was added into the CCPE/pDNA solution to reach a final N/P ratio of 20. After additional 30 min incubation, the CCPE-FA/CCPE/pDNA polyplexes at the N/P ratio of 20 containing different contents of CCPE-FA were prepared.

The ability to bind pDNA of cationic polymers was measured through agarose gel electrophoresis as described in our previous work.²⁴ The sizes and zeta potentials of polyplexes were examined with a Zetasizer Nano ZS (Malvern Instruments, Southborough, MA) by employing the methods as described earlier.³⁰ An atomic force microscopy (AFM) system with a Dimension Icon model and a Nanoscope IIIA controller (Bruker, Santa Barbara, CA) was utilized to visualize the complex morphology. The samples were imaged using the ScanAsyst mode with a setting of 512 pixels per line and a 1 Hz scan rate. Image analysis was performed using Nanoscope software after removing the background slope by flattening images.

Cell viability assay

The MTT assay was performed to evaluate the cytotoxicity of polyplexes in HeLa, C6 and HepG2 cell lines as described earlier.³⁰ The cells were seeded in a 96-well microtiter plate at a density of 10^4 cells per well with $100 \mu\text{L}$ of DMEM per well and kept for 24 h in the incubator. Fresh media containing polyplexes at various N/P ratios were induced into each well to replace the culture media, and the cells were incubated for 4 h continuously. Then, the cells were washed with PBS three times before $100 \mu\text{L}$ of sterile-filtered MTT stock solution (5 mg mL^{-1}) in PBS was added to each well with a final MTT concentration of 0.5 mg mL^{-1} . A Bio-Rad Model 680 Microplate Reader (UK) at a wavelength of 570 nm was used to measure the absorbance of the produced formazan crystals. For each sample, the final absorbance was the average of those measured from six wells in parallel.

In vitro transfection assay

Transfection assays were carried out using plasmid pRL-CMV as the reporter gene in HeLa, C6 and HepG2 cell lines. The cells were seeded in 24-well plates at a density of 5×10^4 cells in $500 \mu\text{L}$ of medium per well and incubated for 24 h. $20 \mu\text{L}$ of polyplexes (containing $1.0 \mu\text{g}$ of pDNA) was added into each well at N/P ratios of 5 to 30. The cells were incubated for 4 h under standard conditions. The medium was replaced with $500 \mu\text{L}$ of fresh normal medium containing 10% FBS. After another 20 h of transfection under the same conditions, the cultured cells were washed twice with PBS and lysed with lysis reagent (Promega Co., Cergy Pontoise, France). A commercial Promega kit and a luminometer (Berthold Lumat LB 9507, Berthold Technologies GmbH. KG, Bad Wildbad, Germany) were used to quantify the luciferase gene expression. Gene expression results were expressed as relative light units (RLUs) per milligram of cell protein lysate ($\text{RLU mg}^{-1} \text{ protein}$). The detailed procedure has been described in our earlier work.^{13,19,30}

To certify the target-specific properties of FA-involved complexes, folate competition assays were performed *via in vitro* gene transfection. The cells were cultured with media that contained free FA with a graded concentration from 0.001 to 0.1 mg mL^{-1} .³³ The other procedure was the same as the gene transfection assay described above.

Gene transfection mediated by polyplexes was also assessed at their optimal N/P ratios using plasmid pEGFP-N1 as the reporter gene in HeLa and HepG2 cells, which was performed using the same procedures as described above. A Leica DML fluorescence microscope was used to image the transfected cells intuitively. The percentage of the EGFP positive cells was determined using flow cytometry (FCM, Beckman Coulter, USA).

Determination of cellular internalization

The cellular internalization rate of polyplexes was evaluated in HeLa and HepG2 cells. The cells were seeded into a 6-well plate at a density of 8×10^5 cells in 3 mL of DMEM per well and incubated for 24 h. Then, 2 mL of DMEM containing 10% FBS without antibiotics was used to replace the medium. The polyplexes containing $6 \mu\text{g}$ of pDNA labeled using the fluorescent dye YOYO-1 were added to each well. After incubation for 4 h, the cells were washed with PBS for about 5 times and trypsinized for flow cytometer study (FACSCalibur). To obtain visual fluorescence images, a Leica DMI3000 B fluorescence microscope was employed to image the cellular internalization of cells, where nuclei were stained blue with 150 ng mL^{-1} DAPI in PBS.

Statistical analysis

All experiments were repeated at least three times. Data was presented as means \pm standard deviation. Statistical significance ($p < 0.05$) was evaluated by using Student's *t*-test when only two groups were compared. If more than two groups were compared, evaluation of significance was performed using

one-way analysis of variance (ANOVA) followed by Bonferroni's *post hoc* test. In all tests, statistical significance was set at $p < 0.05$.

Results and discussion

Preparation of CCPE-FA

In this work, different types of FA-functionalized PAsp polyplexes were prepared based on CCPEs. The detailed synthetic routes of CCPEs are illustrated in Fig. 1. CCPEs were obtained based on the ring-opening reaction of BLA-NCA initiated by the primary amine groups of CCEs, where multiple β -CD units were tied on one CS backbone of CC. The typical ^1H NMR spectra of CS, CC and CCE are shown and analyzed in detail in ESI (Fig. S1†). The used CS chain ($M_n \sim 6.14 \times 10^3 \text{ g mol}^{-1}$, Table 1) contains about 16 primary amine groups (Fig. S1(a)†). For the preparation of CC, some amine groups of CS were reacted with the epoxy groups of CD-EPs, where one CD-EP unit possessed one epoxy ring (Fig. S1(b)†). Based on the molecular weights of CS and CC (Table 1), about four β -CD units were threaded on one CS chain. To produce CCE with more primary amine groups, some hydroxyl groups of CC were directly modified by ED under the activation of CDI. Based on the spectrum of CCE (Fig. S1(c)†), one CCE initiator possessed about 32 primary amine groups to produce a series of CC-graft-PAsps (CCPs) with different lengths of PBLA side chains (Fig. 1). PBLA side chains were subsequently aminolyzed with ED, producing CCPEs with cationic PAsp chains. The lengths

of PAsp chains can be controlled by varying feed ratios of BLA-NCA. Herein, the molar feed ratios [the amino group of CCE]:[BLA-NCA] of 1:30, 1:50, and 1:100 were used to produce CCPE1, CCPE2 and CCPE3, correspondingly. The molecular weights of CCPEs are summarized in Table 1. On increasing the molar feed ratio, the molecular weights of CCPEs increased from 3.07×10^4 to $9.77 \times 10^4 \text{ g mol}^{-1}$. The typical ^1H NMR spectra of CCP and CCPE are shown and analyzed in detail in ESI (Fig. S1†).

FA-functionalized CCPE (CCPE-FA) was obtained *via* a host-guest interaction between the CD units of CCPEs and the Ad species of Ad-FA.^{35,36} The typical ^1H NMR spectra of Ad-FA and CCPE-FA are shown and analyzed in detail in ESI (Fig. S2†). The appearance of signals associated with FA confirmed the successful preparation of CCPE-FA. Based on CCP and CCPE-FA, three types of polyplexes, namely CCP/pDNA, CCPE-FA/pDNA, and ternary CCPE-FA/CCPE/pDNA (prepared by layer-by-layer assembly) polyplexes as shown in Fig. 1, were subsequently prepared for the following studies.

DNA condensation ability of gene vectors

Good pDNA condensation capability is a prerequisite for efficient non-viral gene delivery vectors. In this work, the ability of CCP and CCPE-FA vectors to bind DNA was confirmed by agarose gel electrophoresis, dynamic light scattering and zeta potential measurements. The formation of polyplexes was first testified by their electrophoretic mobility on an agarose gel at various N/P ratios (Fig. 2). The CCE initiator completely inhibited the migration of pDNA at an N/P ratio of 4.

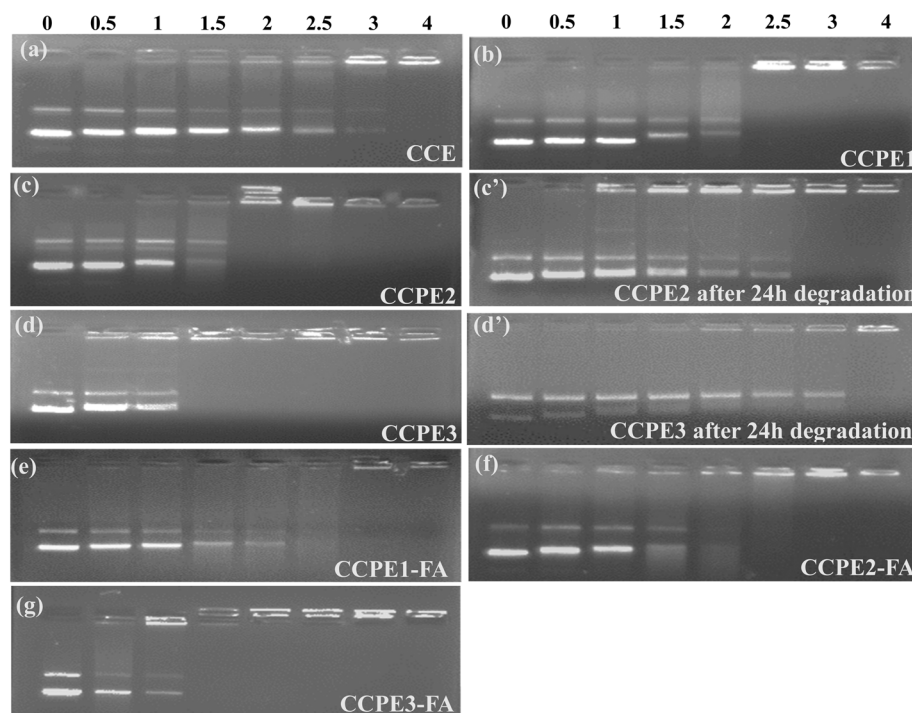


Fig. 2 Electrophoretic mobility of pDNA in the polyplexes of CCE, CCPE and CCPE-FA at various N/P ratios.

All CCPEs exhibited much better pDNA condensation abilities than CCE. In addition, as the molecular weight of polycations increased (Table 1), CCPE3 (prepared with a molar feed ratio [the amino group of CCE]:[BLA-NCA] of 1:100) showed better condensation abilities than CCPE-1 (prepared with a molar feed ratio [the amino group of CCE]:[BLA-NCA] of 1:30). CCPE3 and CCPE1 completely retarded the migration of pDNA at N/P ratios of 1.5 and 2.5, respectively. It is well-known that high-molecular-weight polycations possess better condensation ability.^{19,30} After FA functionalization, CCPE-FA also could condense pDNA efficiently. No appreciable differences were observed in the condensation abilities of CCPE and CCCPE-FA.

Appropriate particle sizes and moderate positive charges benefit the cellular uptake of polyplexes. The particle sizes and zeta potentials of CCPE/pDNA and CCPE-FA/pDNA polyplexes at N/P ratios from 10 to 30 are shown in Fig. 3, where 'gold-standard' polyethylenimine (PEI, $M_w \sim 25$ kDa) was used as the control vector. The particle sizes of polyplexes decreased with increasing N/P ratios (Fig. 3a). When the N/P ratio reached 20, all the particle sizes of polyplexes were within 250 nm, which was suitable for cellular uptake.³⁷ At all N/P

ratios, high-molecular-weight CCPE3/pDNA polyplexes possessed smaller particle sizes than low-molecular-weight CCPE1/pDNA ones. Such results are consistent with their respective DNA condensation capability (Fig. 2). At the same N/P ratio, there were no significant differences between the particle sizes of CCPE-FA/pDNA and CCPE/pDNA polyplexes, further confirming that the introduction of a suitable amount of FA does not obviously affect the condensation capability of CCPE.

Zeta potential is also important in adjusting cellular uptake. As shown in Fig. 3b, in contrast to the particle size trend, the zeta potentials of polyplexes increased with increasing N/P ratios and molecular weights. Polyplexes with positive surface charges are ready to be adsorbed by anionic cell membranes, improving the resulting cellular uptake. In addition, the morphologies of polyplexes were characterized with atomic force microscopy (AFM). Fig. S3 (see ESI†) shows the representative AFM images of (a) CCE/pDNA and (b) CCPE3/pDNA polyplexes at an N/P ratio of 20. CCPE3 can tightly compact DNA into smaller spherical nanoparticles than the starting CCE initiator, which is consistent with their respective DNA condensation capabilities (Fig. 2).

Degradation of PAsp-based vectors

In this work, CCPE3 with a molecular weight of 9.77×10^4 g mol⁻¹ (Table 1) was selected for studying the degradation ability. CCPE3 was dissolved in buffered saline (PBS) solution and incubated at 37 °C. The solutions at different times were sampled and characterized by GPC to obtain the molecular weight of degraded CCPE3. As shown in Fig. 4a, the molecular weight decreased substantially at the initial time of degradation. Fig. 4b demonstrates the significant differences between the aqueous GPC traces of CCPE3 before and after the final degradation. After degradation, the M_n of the final degra-

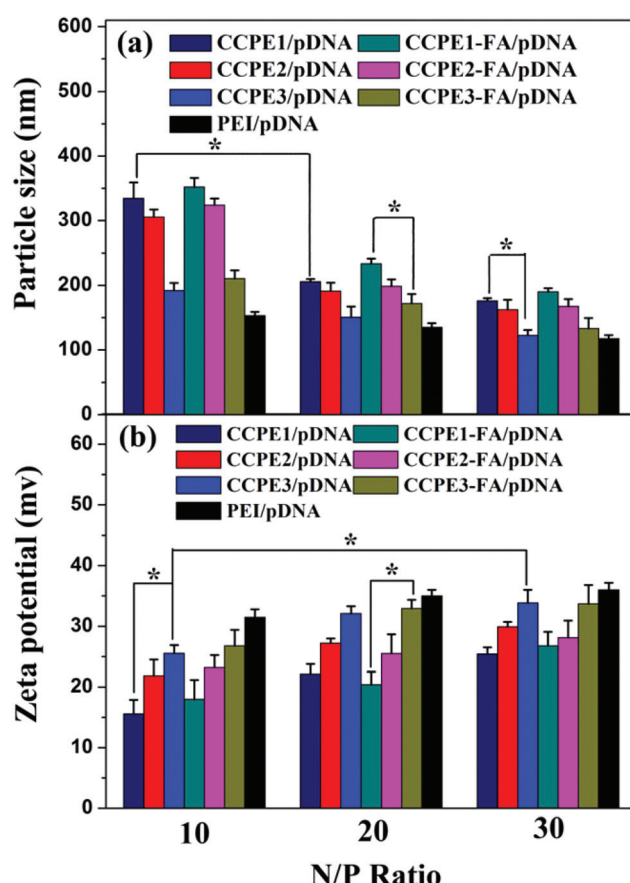


Fig. 3 Particle sizes (a) and zeta potentials (b) of the polymer (CCPE, CCPE-FA and PEI (25 kDa))/pDNA polyplexes at various N/P ratios. Error bars represent the standard deviation (mean \pm SD, $n = 5$). $*p < 0.05$.

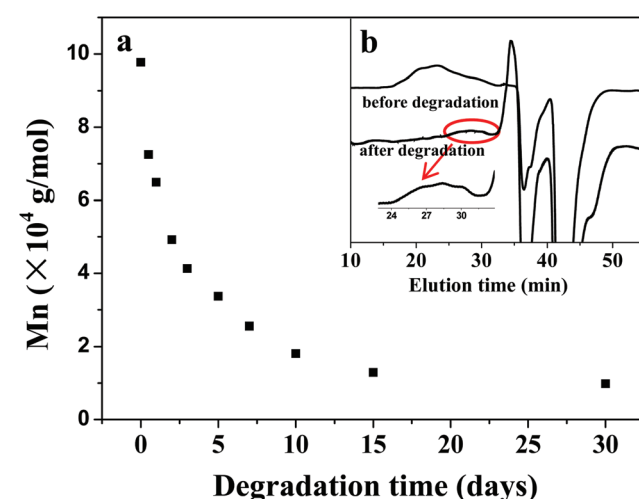


Fig. 4 (a) Molecular weight changes of CCPE3 with degradation time in PBS (pH 7.4) at 37 °C and (b) aqueous GPC traces obtained for CCPE3 before and after degradation.

dation products was near to that of the CCE initiator. The lower peak intensity of the degradation products arose from the very small amount of CCE in CCPE3. The above results confirmed the excellent degradability of PAsp side chains of CCPE.

The degradation of CCPE may be beneficial to pDNA release from polyplexes. As shown in Fig. 2c' and d', the ability of CCPE to condense pDNA was substantially weakened after degradation. The degraded CCPE exhibited a similar condensation ability to that of the CCE initiator (Fig. 2a). In comparison with the tightly compacted polyplexes (Fig. S3b†), degradation caused the CCPE3/pDNA polyplexes to become larger (Fig. S3b'†). Once the polyplexes are taken up by cells, the decreased condensation ability caused by degradation would facilitate the release of pDNA and in turn benefit the resulting gene transfection.

Cytotoxicity assay

The cytotoxicities of CCPE/pDNA and CCPE-FA/pDNA polyplexes in HeLa, C6 and HepG2 cell lines were evaluated *via* the MTT assay in comparison with those of PEI (25 kDa)/pDNA polyplexes (Fig. 5). The cytotoxicities of CCPE/pDNA and CCPE-FA/pDNA polyplexes slightly increased with the increase in N/P ratios. This may be caused by free CCPEs or CCPE-FAs in addition to the compact polyplexes at higher N/P ratios. However, in comparison with PEI, CCPE and CCPE-FA exhibited significantly lower cytotoxicity in all cell lines even at higher N/P ratios. For example, at a given N/P ratio of 30, CCPE and CCPE-FA demonstrated over 70% cell viability, while cell viability treated by PEI/pDNA polyplexes was below 25%. No obvious differences in cell viability were observed between CCPE and CCPE-FA. The lower cytotoxicity of CCPE and CCPE-FA is probably attributed to the biocompatibility of CS and CD, and the biodegradability of PAsp side chains.

Gene transfection assay using CCPE polyplexes

The *in vitro* gene transfection ability was evaluated mainly using luciferase as the reporter gene at various N/P ratios in HeLa, C6 and HepG2 cell lines. Fig. 6 shows the gene transfection efficiencies mediated by CCE/pDNA, CCPE/pDNA and CCPE-FA/pDNA polyplexes at various N/P ratios, which were compared with those of 'gold-standard' PEI (25 kDa) at its optimal N/P ratio of 10.^{29,30,36} For the CCPE and CCPE-FA vectors, their gene transfection efficiencies first increased until the peak values and then decreased slightly with the increase in N/P ratios. At lower N/P ratios, CCPE and CCPE-FA could not tightly compact pDNA. The gene transfection efficiencies of CCPE/pDNA and CCPE-FA/pDNA polyplexes reached the peak values at an N/P ratio of 20. After that, transfection efficiencies decreased slightly at higher N/P ratios where the transfection formulations also contained free CCPE or CCPE-FA as well as the polyplexes. The increased concentration of free CCPE and CCPE-FA slightly increased the cytotoxicity (Fig. 5), probably resulting in a reduction in the transfection performance.

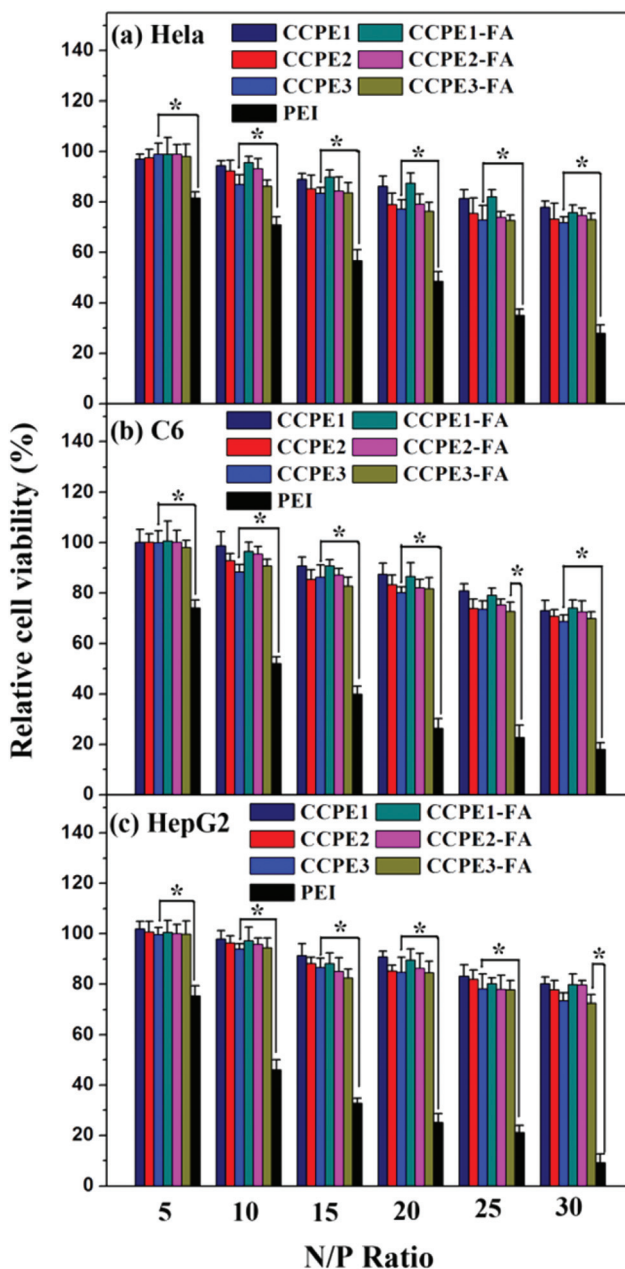


Fig. 5 Cell viabilities of CCPE/pDNA and CCPE-FA polyplexes in comparison with those of branched PEI/pDNA polyplexes at different N/P ratios in (a) HeLa, (b) C6 and (c) HepG2 cell lines. Error bars represent the standard deviation (mean \pm SD, $n = 6$, $*p < 0.05$).

In addition to the N/P ratios, transfection efficiencies are also dependent on the molecular weights of CCPEs (Fig. 6). At most N/P ratios, the increase in transfection efficiencies generally followed the order of CCPE1 < CCPE2 < CCPE3, with pronounced enhancements in CCPE2 and CCPE3. The longer cationic PAsp side chains of CCPE3 could increase the binding ability and complex stability as shown in Fig. 2 and 3, leading to much higher transfection efficiencies.³⁰

As expected, the transfection efficiencies mediated by all CCPEs were significantly higher than those mediated by the

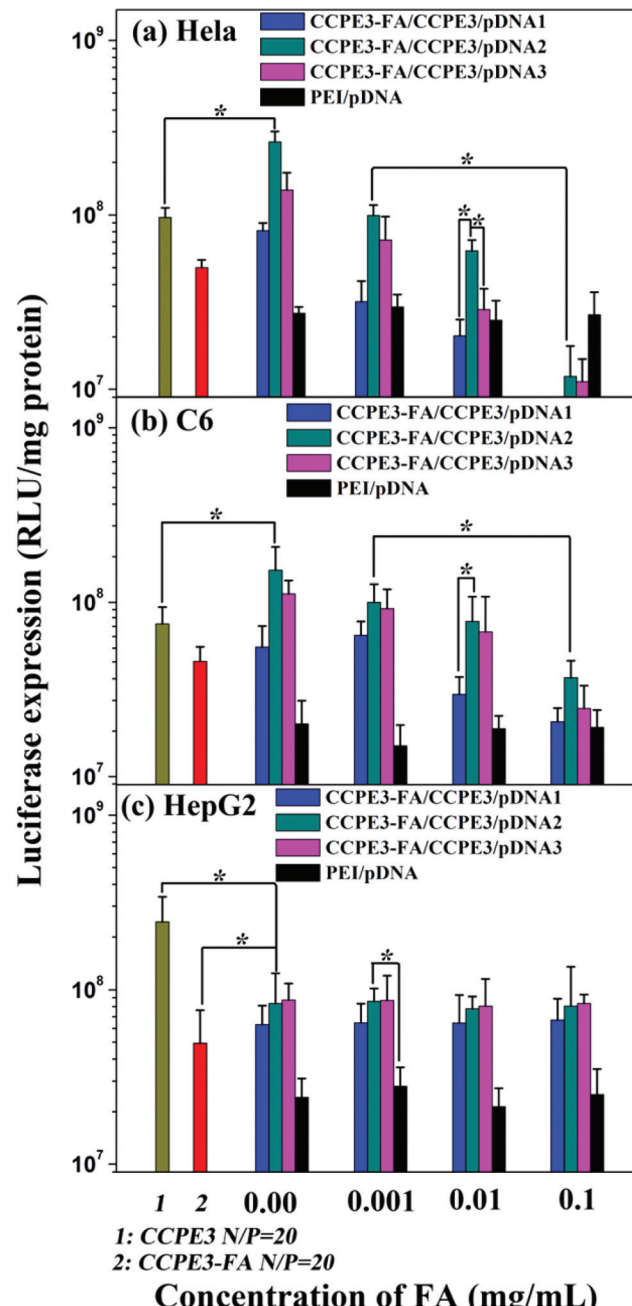
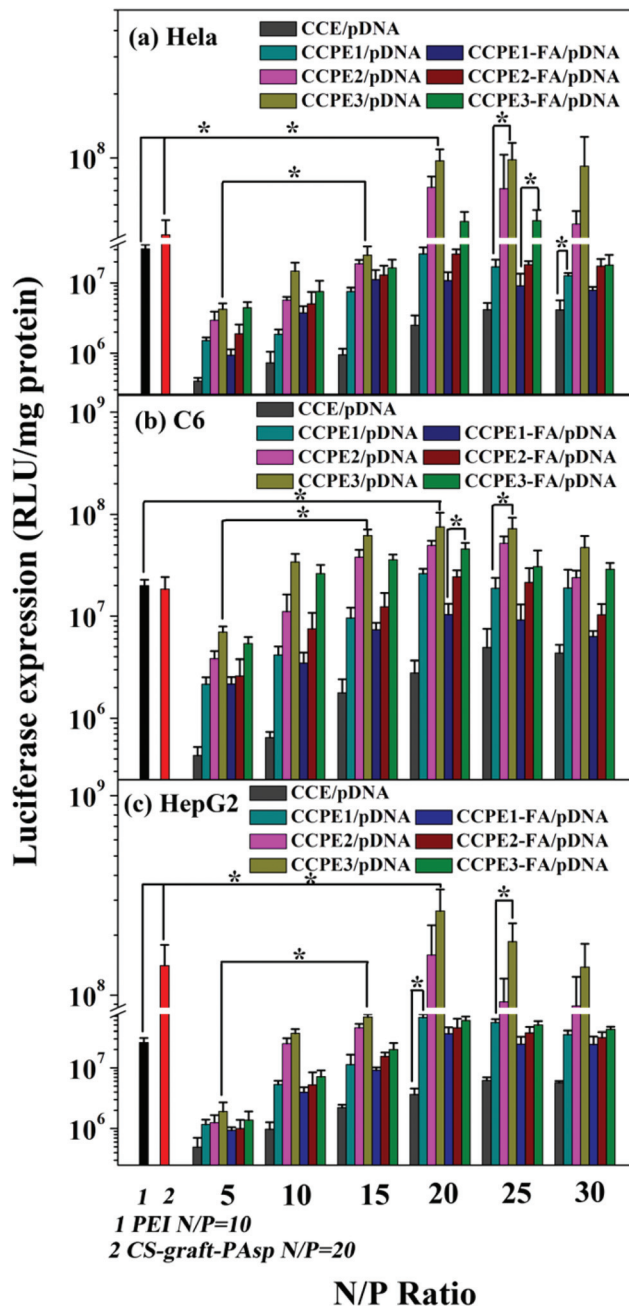


Fig. 6 *In vitro* gene transfection efficiencies mediated by the polyplexes (CCE, CCPE and CCPE-FA) at various N/P ratios in comparison with those of PEI (25 kDa) (at its optimal N/P ratio of 10) in (a) HeLa, (b) C6 and (c) HepG2 cell lines. Error bars represent the standard deviation (mean \pm SD, $n = 3$, * $p < 0.05$).

CCE initiator. As shown in Fig. 2a, CCE possessed a very poor pDNA condensation ability. At most N/P ratios, CCPE2 and CCPE3 produced substantially higher efficiencies than those mediated by PEI at its optimal N/P ratio of 10. The best cationic PAsp side chain-grafted CS (CS-graft-PAsp) ($M_n = 6.37 \times 10^4$ g mol $^{-1}$) reported in our earlier work³⁰ was also selected as the control. The transfection efficiencies mediated by CS-graft-PAsp at its optimal N/P ratio of 20 were investigated in the

three cell lines. As shown in Fig. 6, CCPE2 and CCPE3 exhibited much better gene transfection performances than CS-graft-PAsp in all the HeLa, C6 and HepG2 cell lines. Such results

indicated that in comparison with CS backbones, the CCE backbones with multiple flanking β -CD units were more suitable for constructing highly efficient gene vectors.

Gene transfection assay using FA-involved polyplexes

As mentioned above, after FA functionalization, the introduction of Ad-FA did not obviously affect the condensation capability of CCPE (Fig. 2 and 3). However, as shown in Fig. 6, the transfection efficiency mediated by CCPE-FA was generally lower than that of the corresponding CCPE counterpart in both folate receptor (FR)-positive (HeLa and C6) and negative (HepG2) cells. Gene transfection is a complex process involving the cellular uptake of polyplexes, pDNA escape from lysosome, nuclear targeting/entry, as well as condensation ability. CCPE-FA was produced by host-guest interactions between the β -CD units of CCPE and the Ad species of Ad-FA. Ad-FA was packed into the whole polyplexes, where the introduced Ad-FA species may hinder the pDNA escape from polyplexes in cells and consequently lead to a lower transfection efficiency.

In order to obtain effective targeting properties of FA, the ternary polyplexes of CCPE-FA/CCPE/pDNA were prepared by layer-by-layer assembly (Fig. 1). Instead of FA involvement in the whole polyplexes (Fig. 6), FA in the ternary polyplexes was only packed in the outer layer, reducing the possible effect of Ad-FA on pDNA escape processes after cellular uptake. Due to its best performance among CCPEs, CCPE3 was selected for the preparation of ternary polyplexes. As shown in Fig. 6, CCPE3 and CCPE3-FA exhibited the optimal transfection

efficiencies at an N/P ratio of 20. In this work, different ternary CCPE3-FA/CCPE3/pDNA1, CCPE3-FA/CCPE3/pDNA2 and CCPE3-FA/CCPE3/pDNA3 polyplexes with a final N/P ratio of 20 were prepared. The corresponding CCPE3/pDNA pre-polyplexes were first prepared at the respective N/P ratios of 5, 10 and 15. Then a suitable amount of CCPE-FA was added to reach the final N/P ratio of 20. As shown in Fig. 7, in the absence of free FA, all ternary CCPE3-FA/CCPE3/pDNA polyplexes showed much higher gene transfection efficiencies than their CCPE3-FA/pDNA counterparts in the FR-positive HeLa and C6 cell lines. For the CCPE3-FA/pDNA complexes, the FA ligands were into the whole polyplexes, thus the targeting group cannot be effectively identified by FA-acceptors on the surface of cell membrane. In addition, as discussed above, the whole entrapment of Ad-FA hindered pDNA escape. For ternary CCPE3-FA/CCPE3/pDNA polyplexes, FA was only introduced into the outer layer, making the identification of FA-acceptors in the polyplexes easier as well as reducing the possible effect of Ad-FA on pDNA escape processes.

In particular, the gene transfection performance mediated by CCPE3-FA/CCPE3/pDNA2 largely exceeded that of CCPE3/pDNA. As shown in Fig. S4 (see ESI†), no obvious changes were presented in respect of particle sizes and zeta potentials among the ternary CCPE3-FA/CCPE3/pDNA polyplexes. CCPE3-FA/CCPE3/pDNA1 contained more contents of Ad-FA, which did not benefit the gene transfection process as confirmed in Fig. 6 by using CCPE3-FA/pDNA. CCPE3-FA/CCPE3/pDNA3 possessed a smaller amount of Ad-FA, which might not make the

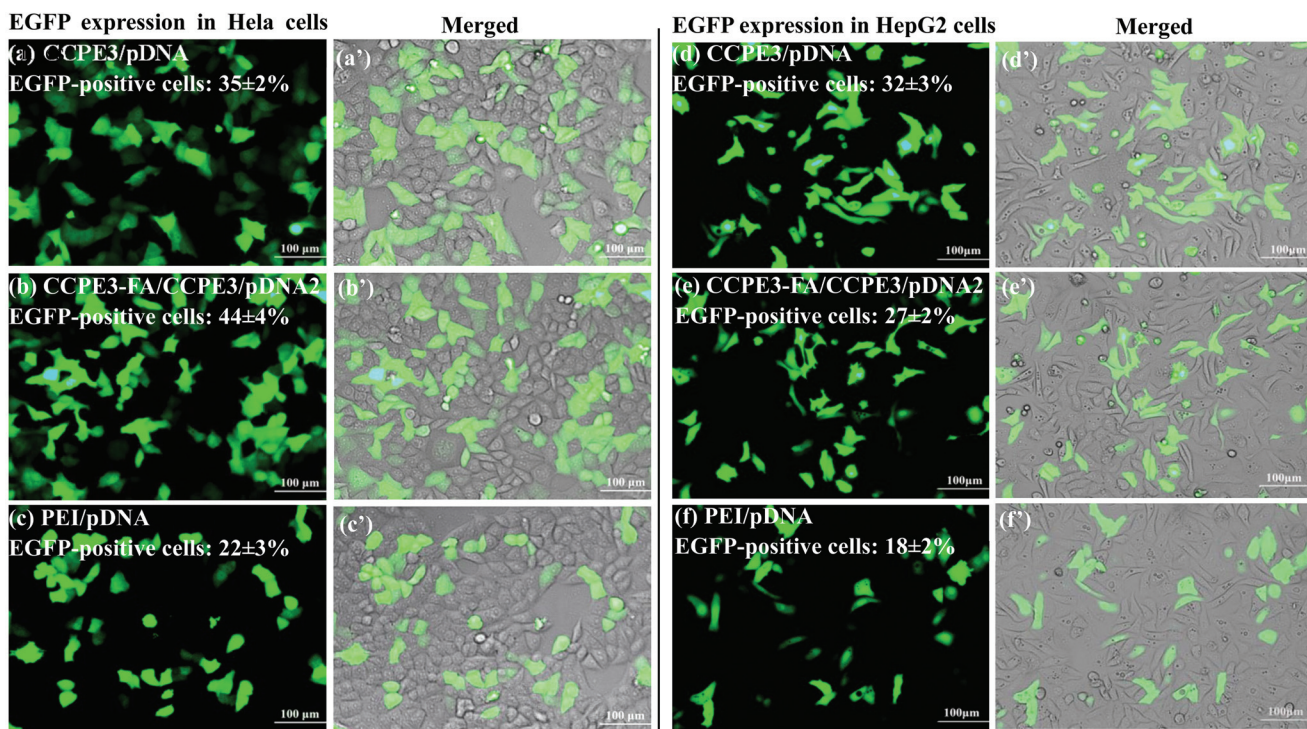


Fig. 8 EGFP expression mediated by CCPE3/pDNA and CCPE3-FA/CCPE3/pDNA2 polyplexes at an N/P ratio of 20 and PEI/pDNA polyplexes at an N/P ratio of 10 in (a–c) HeLa cell lines and (d–f) HepG2 cell lines.

target-specific properties of FA work well. Thus, CCPE3-FA/CCPE3/pDNA2 with a modest amount of Ad-FA demonstrated the best results in the FR-positive cell lines. However, in FR-negative HepG2 cell lines, the transfection efficiencies of all ternary polyplexes were still much lower than that of CCPE3/pDNA. No significant differences were observed between the CCPE3-FA/CCPE3/pDNA and CCPE3-FA/pDNA polyplexes. The above results indicated that in ligand receptor-positive cell lines, the introduction of a suitable amount of ligand by layer-by-layer assembly could enhance the transfection performance of polyplexes.

To further confirm the target-specific properties of ternary CCPE3-FA/CCPE3/pDNA polyplexes, folate competition assays were performed in the FR-positive and negative cell lines. The transfection procedure was the same as described above except that the culture medium contained free FA with graded concentrations from 0.001 to 0.1 mg mL⁻¹. As shown in Fig. 7, in the FR-positive HeLa and C6 cell lines, the transfection efficiencies of all ternary CCPE3-FA/CCPE3/pDNA polyplexes

significantly decreased with the increase in the concentration of free FA. No obvious changes were observed in the control PEI/pDNA polyplexes. The above results indicated that free FA affected the transfection efficiencies of FA-involved ternary polyplexes. On the other hand, in the FR-negative HepG2 cell lines, the ternary CCPE3-FA/CCPE3/pDNA polyplex maintained similar transfection efficiencies regardless of free FA concentrations. The results indicated that the FA-involved ternary polyplexes possessed the FR-positive cancer-targeting properties.

To intuitively verify the good transfection performance of ternary CCPE3-FA/CCPE3/pDNA2 polyplexes, plasmid pEGFP-N1 encoding enhanced green fluorescent protein (EGFP) was also used in this work in HeLa and HepG2 cells. Fig. 8 shows the representative fluorescence microscopic images of EGFP expression mediated by the CCPE3/pDNA and CCPE3-FA/CCPE3/pDNA2 (at the optimal N/P ratio of 20) and control PEI/pDNA (at the N/P ratio of 10) polyplexes. CCPE3/pDNA and CCPE3-FA/CCPE3/pDNA2 demonstrated significantly stronger fluorescence signals in comparison with PEI in

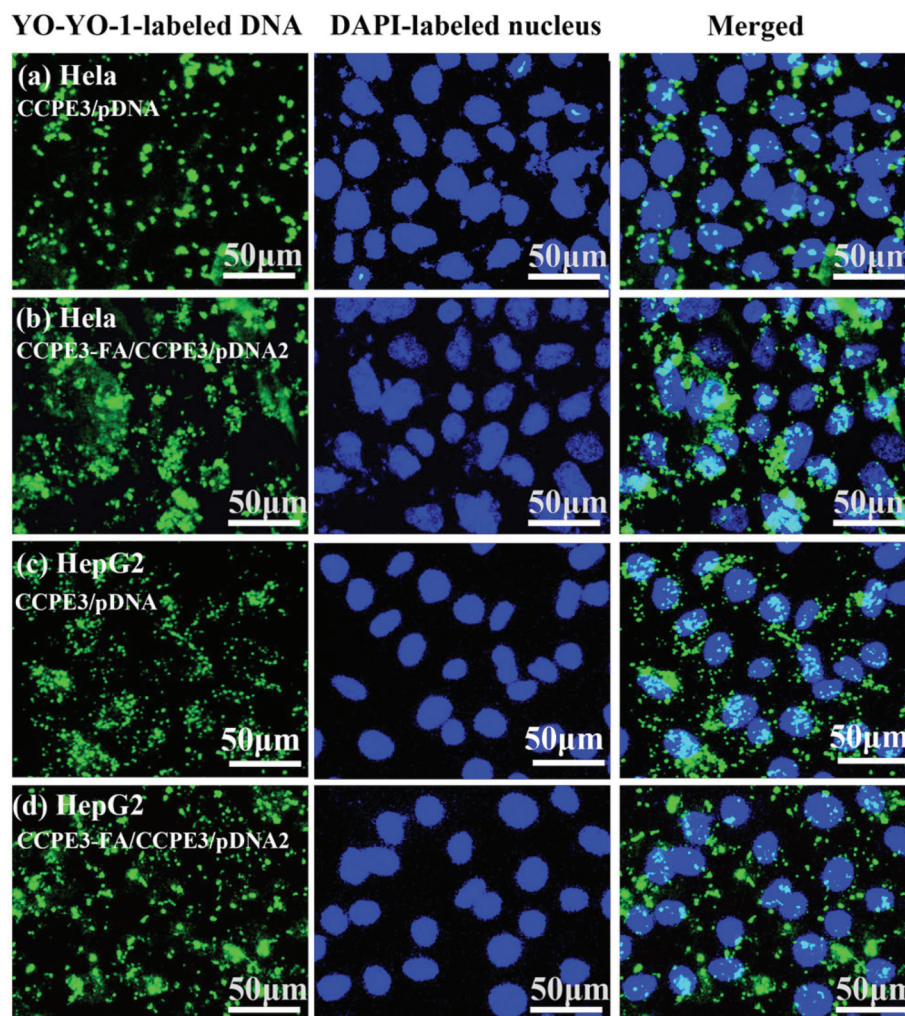


Fig. 9 Fluorescence images of HeLa and HepG2 cells treated with CCPE3/pDNA and CCPE3-FA/CCPE3/pDNA2 polyplexes for 4 h, where the YOYO-1-labeled pDNA is shown in green, and the DAPI-labeled nucleus is shown in blue.

both FR-positive HeLa and FR-negative HepG2 cells. Nevertheless, in the FR-positive HeLa cells, CCPE3-FA/CPPE3/pDNA2 exhibited much stronger fluorescence signals than CCPE3/pDNA. The percentage of positive-EGFP cells presenting transfection efficiency was calculated with flow cytometry. CCPE3/pDNA and CCPE3-FA/CCPE3/pDNA2 exhibited the percentages of 35% and 44% for HeLa cells (or 32% and 27% for HepG2 cells), respectively, while PEI/pDNA showed a lower percentage of 22% for HeLa cells (or 18% for HepG2 cells). The above results are consistent with those of Fig. 7.

Cellular internalization

The cellular internalization of CCPE3/pDNA and CCPE3-FA/CCPE3/pDNA2 polyplexes at an N/P ratio of 20 was observed after 4 h incubation in HeLa and HepG2 cell line, where pDNA was labeled in green and the nucleus was stained blue. Fig. 9 reveals that compared with CCPE3/pDNA, more pDNA polyplexes aggregated within the HeLa cells treated with CCPE3-FA/CCPE3/pDNA2. In the FR-negative HepG2 cells, there were no obvious differences between CCPE3/pDNA and CCPE3-FA/CCPE3/pDNA2. The cellular internalization of polyplexes was quantified by flow cytometry. As shown in Fig. S5 (see ESI†), CCPE3/pDNA and CCPE3-FA/CCPE3/pDNA demonstrated the cellular internalization rates of 77.5% and 94.3% for HeLa cells (or 88.8% and 82.4% for HepG2 cells), respectively. In the FR-positive HeLa cells, FA introduction in CCPE3-FA/CCPE3/pDNA facilitated the cellular uptake. Higher cellular internalization of polyplexes would benefit the resulting gene transfection. The results of cellular internalization are consistent with those of transfection efficiencies as shown in Fig. 7 and 8.

Conclusions

Different types of FA-functionalized degradable polyplexes were successfully prepared based on the PAsps-grafted CC conjugate (CCPE), where multiple β -CD units were tied on a CS chain. FA-functionalized CCPE (*i.e.* CCPE-FA) was readily prepared by host–guest interactions between β -CD units of CCPE and Ad species of Ad-FA. The resulting CCPE/pDNA, CCPE-FA/pDNA, and ternary CCPE-FA/CCPE/pDNA (prepared by layer-by-layer assembly) polyplexes were compared systematically in FR-positive HeLa and C6 cells and FR-negative HepG2 cells. The CCPE/pDNA polyplexes produced much higher transfection efficiencies than the cationic PAsp chain-grafted CS based polyplexes. Ternary CCPE-FA/CCPE/pDNA polyplexes with suitable amounts of ligands demonstrated excellent gene transfection abilities in the FR-positive tumor cells. The present work would offer a promising strategy for designing highly efficient ligand-functionalized degradable polyplexes.

Acknowledgements

This work was partially supported by the National Natural Science Foundation of China (grant numbers 51173014,

51221002, 51325304, 51473014, 81171682, and 31430030), Opening Project of State Key Laboratory of Polymer Materials Engineering (Sichuan University) (grant number sklpme2014-4-23) and Collaborative Innovation Center for Cardiovascular Disorders, Beijing Anzhen Hospital affiliated to the Capital Medical University.

Notes and references

- 1 L. Novo, E. Mastrobattista, C. F. van Nostrum and W. E. Hennink, *Bioconjugate Chem.*, 2014, **25**, 802.
- 2 H. Tian, L. Lin, J. Chen, X. Chen, T. G. Park and A. Maruyama, *J. Controlled Release*, 2011, **155**, 47.
- 3 F. J. Xu and W. T. Yang, *Prog. Polym. Sci.*, 2011, **36**, 1099.
- 4 H. C. Kang, K. M. Huh and Y. H. Bae, *J. Controlled Release*, 2012, **164**, 256.
- 5 P. Chan, M. Kurisawa, J. E. Chung and Y. Y. Yang, *Biomaterials*, 2007, **28**, 540.
- 6 A. A. Eltoukhy, D. Chen, C. A. Alabi, R. Langer and D. G. Anderson, *Adv. Mater.*, 2013, **25**, 1487.
- 7 C. Zhang, S. Gao, W. Jiang, S. Lin, F. Du, Z. Li and W. Huang, *Biomaterials*, 2010, **31**, 6075.
- 8 M. A. Islam, T. E. Park, B. Singh, S. Maharjan, J. Firdous, M. H. Cho, S. K. Kang, C. H. Yun, Y. J. Choi and C. S. Cho, *J. Controlled Release*, 2014, **193**, 74.
- 9 J. C. Fernandes, X. Qiu, F. M. Winnik, M. Benderdour, X. Zhang, K. Dai and Q. Shi, *Int. J. Nanomed.*, 2012, **7**, 5833.
- 10 W. Sajomsang, P. Gonil, U. R. Ruktanonchai, M. Petchsangsai, P. Opanasopit and S. Puttipipatkhachorn, *Carbohydr. Polym.*, 2013, **91**, 508.
- 11 B. Layek and J. Singh, *Biomacromolecules*, 2013, **14**, 485.
- 12 X. Zhao, Z. Li, H. Pan, W. Liu, M. Lv, F. Leung and W. W. Lu, *Acta Biomater.*, 2013, **9**, 6694.
- 13 Y. Ping, C. D. Liu, J. S. Li, J. Li, G. P. Tang, W. T. Yang and F. J. Xu, *Adv. Funct. Mater.*, 2010, **20**, 3106.
- 14 J. Li, C. Yang, H. Li, X. Wang, S. H. Goh, J. L. Ding, D. Y. Wang and K. W. Leong, *Adv. Mater.*, 2006, **18**, 2969.
- 15 C. O. Mellet, J. M. G. Fernández and J. M. Benito, *Chem. Soc. Rev.*, 2011, **40**, 1586.
- 16 C. Y. Quan, J. X. Chen, H. Y. Wang, L. Cao, C. Chang, X. Z. Zhang and R. X. Zhuo, *ACS Nano*, 2010, **4**, 4211.
- 17 Z. H. Wang, Y. Zhu, M. Y. Chai, W. T. Yang and F. J. Xu, *Biomaterials*, 2012, **3**, 1873.
- 18 Q. Tang, B. Cao, X. Lei, B. Sun, Y. Q. Zhang and G. Cheng, *Langmuir*, 2014, **30**, 5202.
- 19 X. C. Yang, Y. L. Niu, N. N. Zhao, C. Mao and F. J. Xu, *Biomaterials*, 2014, **35**, 3873.
- 20 Y. L. Lo, Y. S. Wang and L. F. Wang, *Adv. Healthcare Mater.*, 2013, **2**, 1458.
- 21 Y. Y. He, Y. Nie, G. Cheng, L. Xie, Y. Q. Shen and Z. W. Gu, *Adv. Mater.*, 2013, **26**, 1534.
- 22 L. Chen, T. Jiang, C. Cai, L. Wang, J. Lin and X. Cao, *Adv. Healthcare Mater.*, 2014, **3**, 1508.
- 23 J. Gu, X. Chen, H. Xin, X. Fang and X. Sha, *Int. J. Pharm.*, 2014, **461**, 559.

- 24 X. B. Dou, Y. Hu, N. N. Zhao and F. J. Xu, *Biomaterials*, 2014, **35**, 3015.
- 25 T. Akagi, F. Shima and M. Akashi, *Biomaterials*, 2011, **32**, 4959.
- 26 J. Shen, D. J. Zhao, W. Li, Q. L. Hu, Q. W. Wang, F. J. Xu and G. P. Tang, *Biomaterials*, 2013, **34**, 4520.
- 27 K. Miyata, M. Oba, M. Nakanishi, S. Fukushima, Y. Yamasaki, H. Koyama, N. Nishiyama and K. Kataoka, *J. Am. Chem. Soc.*, 2008, **130**, 16287.
- 28 C. Li, F. Zhao, Y. Huang, X. Liu, Y. Liu, R. Qiao and Y. Zhao, *Bioconjugate Chem.*, 2012, **23**, 1832.
- 29 J. J. Nie, X. B. Dou, H. Hu, Y. Hu, B. R. Yu and F. J. Xu, *ACS Appl. Mater. Interfaces*, 2015, **7**, 553.
- 30 H. Q. Song, X. B. Dou, R. Q. Li, B. R. Yu, N. N. Zhao and F. J. Xu, *Acta Biomater.*, 2015, **12**, 156.
- 31 A. Galbiati, C. Tabolacci, B. Morozzo Della Rocca, P. Mattioli, S. Beninati, G. Paradossi and A. Desideri, *Bioconjugate Chem.*, 2011, **22**, 1066.
- 32 F. Zhao, H. Yin, Z. Zhang and J. Li, *Biomacromolecules*, 2013, **14**, 476.
- 33 L. Sun, Z. Wei, H. Chen, J. Liu, J. Guo, M. Cao, T. Wen and L. Shi, *Nanoscale*, 2014, **6**, 8878.
- 34 Z. Gao and X. Zhao, *Polymer*, 2004, **45**, 1609.
- 35 C. Y. Ang, S. Y. Tan, X. Wang, Q. Zhang, M. Khan, L. Bai, S. T. Selvan, X. Ma, L. Zhu, K. T. Nguyen, N. S. Tan and Y. Zhao, *J. Mater. Chem. B*, 2014, **2**, 1879.
- 36 Y. Hu, M. Y. Chai, W. T. Yang and F. J. Xu, *Bioconjugate Chem.*, 2013, **24**, 1049.
- 37 P. van de Wetering, E. E. Moret, N. M. E. Schuurmans-Nieuwenbroek, M. J. van Steenbergen and W. E. Hennink, *Bioconjugate Chem.*, 1999, **10**, 589.